Quantitative ^{131}I SPECT with Triple Energy Window Compton Scatter Correction

Yuni Dewaraja, Jia Li and Kenneth Koral
Division of Nuclear Medicine, University of Michigan Medical Center, Ann Arbor, MI 48109-0552

Abstract

In this work accuracy of quantitative ^{131}I SPECT with triple energy window (TEW) scatter correction is evaluated by phantom measurements. The TEW method is a pixel by pixel correction where the scatter fraction in the photopeak window is estimated by linear interpolation between two adjacent narrow sub-windows. Quantification procedure includes marker based X-ray CT-SPECT image fusion to determine object boundaries and to generate attenuation maps. TEW scatter correction significantly reduces the effect of background activity on reconstructed counts within an object, but it still exists due to the finite position resolution of the system. Therefore, a background dependent calibration factor was used for quantification. Quantitative accuracy with TEW correction was 5% and 14% for a tumor and lung respectively of a physical phantom with non-uniform activity and non-uniform scattering medium.

I. INTRODUCTION

Quantitative single photon emission computed tomography (SPECT) is being performed for tumor dosimetry of B-cell lymphoma patients treated with ^{131}I radioimmunotherapy. Accurate quantification in SPECT requires correction for both attenuation and scatter. Scatter correction is necessary because counts accepted by the photopeak window will include photons that have undergone Compton scatter in the patient or collimator. Scattered photons have lost part of their energy prior to reaching the detector but, a significant fraction deposit sufficient energy in the detector for the pulse height to be within the typical 10-20% photopeak window. These scattered photons degrade the image contrast and results in erroneous tumor quantification because of the increase in the measured counts. The amount of scatter depends on the distribution of the scatterer as well as on the source distribution and energy.

Several scatter compensation techniques such as deconvolution methods, multiple energy window methods and spectral-fitting methods have been investigated for SPECT imaging with ^{99m}Tc. Recently, commonly used scatter correction techniques for ^{99m}Tc have been compared using Monte Carlo simulation[1][2]. Literature on scatter correction for ^{131}I SPECT is very limited[3]. Photopeak contamination in ^{131}I imaging is more significant than in ^{99m}Tc due to the higher energy of the peak (364 keV compared with 140 keV for ^{99m}Tc) and also due to the multiple gamma ray emissions. Two of the ^{131}I emissions are at 637 keV (6.5%) and 723 keV (1.7%) and therefore events accepted by the 364 keV (82%) photopeak will include these higher energy photons that have undergone scatter.

The triple energy window (TEW) scatter correction method reported by Ogawa[4][5] has demonstrated good quantitative accuracy for ^{99m}Tc and is practical to implement in a clinic where cameras with multiple window acquisition capability are now commonly available. Prior to this work, ^{131}I scatter correction in our clinic has been done using the dual window or k value method [6]. Unlike the k value method, where a fixed scatter fraction is assumed, the TEW method is a position dependent correction since a scatter fraction is estimated for each pixel. This is desired since the shape of the scattered photon energy spectrum varies from pixel to pixel in the projection images. Also, the TEW method is easier to implement compared to the k value method because a system specific calibration is not required.

Monte Carlo simulation is ideal for assessing scatter correction since it allows for separate tracking of primary and scattered photons. However, a suitable Monte Carlo code for ^{131}I SPECT is not presently available because of the difficulties associated with accurately modeling collimator scatter and penetration which become significant for higher energy gamma-rays. In this work, TEW scatter correction for ^{131}I is evaluated experimentally by quantitative phantom data. A preliminary clinical evaluation is also presented.

II. TEW SCATTER CORRECTION METHOD

Since the scatter spectrum cannot be measured experimentally, the triple energy window method estimates the scatter fraction in the photopeak from the counts acquired in two adjacent narrow windows. Linear interpolation between the two sub-windows (Figure 1) can be used to obtain the following trapezoidal approximation of the scatter counts:

$$C_{scatt} = \left(\frac{C_{low}}{W_{low}} + \frac{C_{high}}{W_{high}} \right) \frac{W_{main}}{2} \qquad (1)$$

where C_{scatt}=scattered photon counts in the photopeak window, C_{low}=counts in the low energy sub-window, C_{high}=counts in the high energy sub-window, W_{low}=width of the low energy sub-window, W_{high}=width of the high energy sub-window and W_{main}=width of the photopeak window.

At each pixel the scattered photons are estimated as above and are subtracted from the total counts measured in the photopeak to obtain the unscattered photons. The TEW correction is appropriate if the trapezoidal estimate of the area is close to the true area under the spectrum of scattered photons. Monte Carlo simulations for ^{99m}Tc typically show the scattered photon spectrum as having a 'S shape' in the photopeak window, resulting in reasonable agreement between the trapezoidal estimate of the scatter counts and the true number of scatter counts[1][2]. When applying TEW correction for ^{99m}Tc the higher energy sub-window can be ignored because the spectrum approaches zero above the photopeak. In ^{131}I imaging however, the high energy window is essential to account for penetration events originating from the 637 and 723 keV photons.

0-7803-4258-5/98/$10.00 © 1998 IEEE

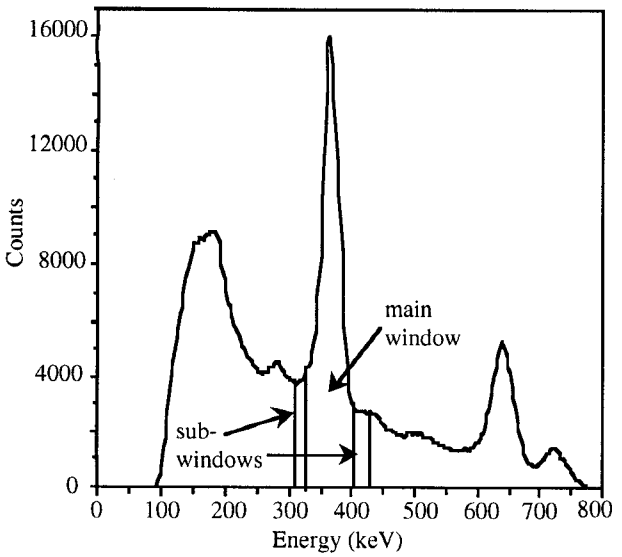

Figure 1: Measured ^{131}I gamma-ray spectrum for a point source in air 19 cm away from collimator.

The correction can be sensitive to statistical fluctuations because of the low number of counts that will be recorded in the narrow sub-windows. Another source of noise is energy spectrum fluctuations due to unstable photomultiplier tubes. When choosing the width and position of the two narrow windows both noise and the accurate estimation of scatter counts must be considered.

III. PHANTOM EXPERIMENTS

All experiments were performed with a Picker Prism 3000 three headed SPECT camera which has three window acquisition capability and high energy parallel hole collimators. Acquisitions employed 360°, a 64x64 matrix, 60 angles and 80-240 sec per angle. For each camera head, the windows were determined by observing the spectrum from a ^{131}I point source in air. Figure 1 shows the measured spectrum and the positioning of the windows. The main window width at 364 keV was set at 20% (72.8 keV) and the two adjacent sub-windows at 6% (low energy sub-window 19 keV, high energy sub-window 25 keV).

Following the same quantification procedure which has been described previously[7], SPECT images and X-ray computed tomography (CT) images were superimposed based on external markers using a registration computer code. The CT-SPECT fusion is used to generate attenuation maps for the space alternating generalized EM reconstruction[8] and to define the object boundaries. Gaussian smoothing was performed on the sub-window projection data. All projection data were dead time corrected based on a ^{131}I decaying source measurement performed with the same triple windows used here. Since the count rates were kept low, the dead time correction was only 1-3%. After the scatter counts in each pixel of the projection data are calculated as given by equation 1, TEW scatter compensation is performed during the reconstruction step prior to attenuation correction. For comparison images were also reconstructed without scatter compensation. The physical object boundaries or regions of interest (ROI) were drawn on the CT images and transferred on to the SPECT images which had been mapped to the CT space. The CT slice thickness was 1 cm and the matrix size was 256x256.

A. Calibration Phantom Measurements

Since the objective is to quantitate tumors (hot spots), a high activity sphere centered in a low activity elliptical phantom was used for the calibration. Both the sphere and the elliptical phantom were filled with water and injected with ^{131}I solution. The sphere volume and activity were 200 cm^3 and 400 μCi while the phantom (background) volume was 8600 cm^3. In order to investigate the effect of background activity on the sphere counts the measurement was performed at three different levels of the background to sphere activity concentration ratio, b: 0, 1/5 and 1/4. the background activity was increased by injecting additional ^{131}I into the elliptical phantom while all other conditions remained the same.

To determine the precision of the quantification procedure with TEW scatter correction the measurement with b=1/5 was repeated on two consecutive days. The calibration was also performed at two different values of the radius of rotation to allow for interpolation when analyzing patients

B. Lung Phantom Measurement

The accuracy of the quantification was evaluated using a physical lung phantom with a 200 cm^3 sphere inserted between the lungs to simulate a tumor. The elliptical lung phantom consisted of the water filled tumor, lungs filled with a mixture of water and Styrofoam beads, backbone made of bone equivalent material and a water filled background. This phantom provides a non-uniform scattering medium. To determine the accuracy of the quantification procedure with uniform and non-uniform background activity distribution two measurements were performed. In the first case the lungs and the background water surrounding the tumor were uniform in activity while in the second measurement non-uniformity was introduced by injecting additional ^{131}I into the left lung. The relative activity concentrations for the first measurement was: tumor, 1.0; right lung, 0.2 ; left lung, 0.2; background, 0.2; backbone, 0;. The only difference in the second measurement was that the right lung relative concentration was increased to 0.5.

For all phantom measurements the counts in the low energy sub-window were 15-16% of the main window counts while the counts in the high energy sub-window were 11-13% of the main window counts. The trapezoidal estimate of scattered counts was close to one half of the total photopeak window counts.

IV. RESULTS

A. Calibration Phantom Results

Using the counts in the reconstructed image sphere ROI a calibration factor, CF, that relates reconstructed counts to activity was obtained. The CF was measured for each camera head both with TEW correction and with no correction. Figure 2 is a plot of the calibration factor for head 1 at the three different levels of measured background to sphere activity concentration ratio, b_{meas}.

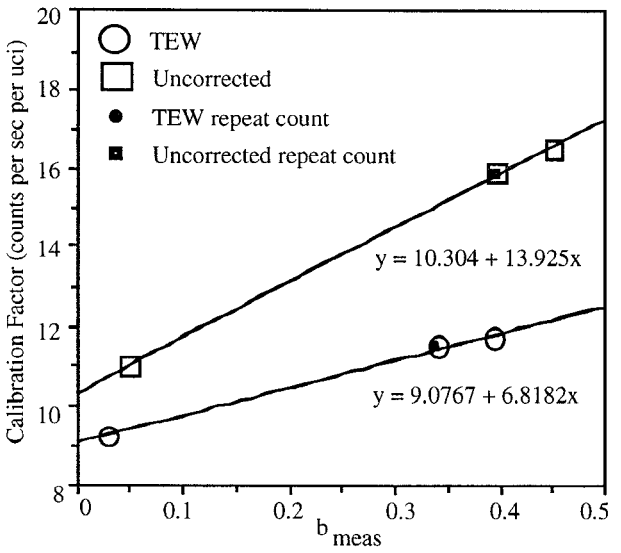

Figure 2: Calibration factor as a function of measured background to sphere activity concentration ratio with and without TEW scatter correction.

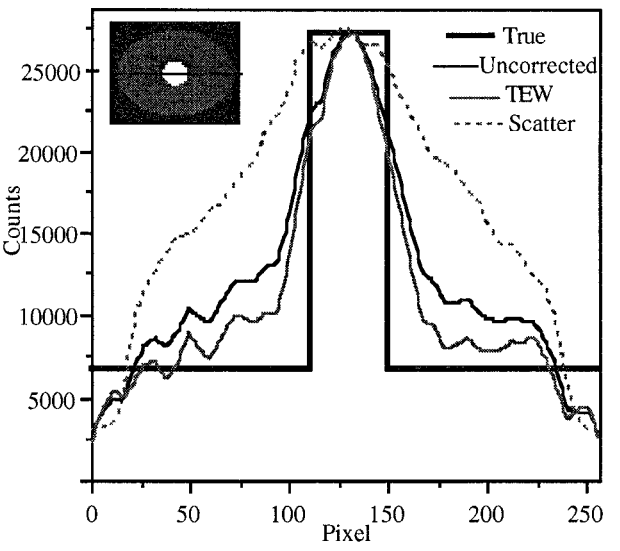

Figure 3: Profile curves along a reconstructed slice of the calibration phantom. Inset shows the true image.

With no scatter correction the sharp increase in the sphere counts with background is to be expected because as the background activity increases more photons will scatter and be included within the sphere ROI increasing its apparent activity. Ideally, after scatter correction the calibration factor should be independent of the background activity. This is not achieved because counts originating outside the sphere will contribute to the sphere ROI counts due to the finite position resolution of the system. It is also possible that the TEW correction is undercompensating for scatter as the background activity increases. This could be easily investigated by a Monte Carlo simulation if a suitable code for ^{131}I were available. The effect of surrounding activity is especially significant in the present work since object boundaries are defined by tight ROI's outlined on the CT. The variation of calibration factor with background activity complicates the tumor quantification procedure in patients since the background to tumor activity concentration ratio is patient dependent. Quantification will involve measuring b for each tumor and obtaining the correct CF to be used from the plot of Figure 2. Examining the slopes of Figure 2 it is evident that TEW scatter correction significantly reduces the dependence of calibration factor on background compared to the uncorrected results.

The counts per sec per μCi obtained for the repeat measurement (performed at b=1/5 only) is also plotted in Figure 2. The two measurements varied by 0.4% with TEW correction and by less than 0.1% with no scatter correction. This result shows that it is possible to get good precision with the present TEW scatter correction although as expected the uncorrected data is less noisy.

Figure 3 shows the intensity profile for a line through the sphere in a reconstructed slice of the calibration phantom (background to sphere activity concentration ratio = 1/4). The true activity distribution is plotted together with the uncorrected profile, the TEW corrected profile and the profile of the image obtained by reconstructing only the trapezoidal estimate of scatter counts. All profiles have been normalized to have the same intensity at the center of the sphere. The scatter corrected profile is closer to the true activity distribution compared to the uncorrected profile but is still significantly different due to the finite position resolution of the system. The loss of contrast due to scatter is evident in the broad profile of the scatter only image.

B. Lung Phantom Results

Figure 4 shows a reconstructed slice of the lung phantom with no scatter correction, the same slice with TEW scatter correction and the estimated scatter only image. The true activity distribution and the X-ray CT of the slice are also shown. The black circle in the SPECT images is the tumor ROI drawn on the CT and transferred to the SPECT images. The scatter corrected image is closer to the true activity distribution compared to the uncorrected image although the difference is subtle. However, the scatter only image of Figure 4(e) differs significantly from the true activity distribution. In this case the low density lungs where Compton scatter probability is relatively low have low intensity, while the backbone where scattering probability is high appears with an intensity as high as the inserted tumor (note true backbone activity is zero).

To determine quantitative accuracy the tumor and right lung activities were calculated and compared to the known true activities. The measured values of background to object activity concentration ratio were 0.3 for the tumor and 1.4 for the lung. The corresponding values of the calibration factor were obtained from the plot of CF vs. b (Figure 2) and used to get the activities shown in Table 1 for both uncorrected and TEW corrected images. Note the difference in true tumor activity between the uniform and non-uniform background conditions is only due to decay between measurements. As the results show in all cases better quantitative accuracy is achieved with TEW scatter correction. For the tumor where object size, shape and medium was same as the calibration sphere the percentage error from true activity was 5.4%. For the lung where object size, shape and medium was significantly different from the calibration sphere the error was 14.4%. The higher error in the case of the lung could be due to

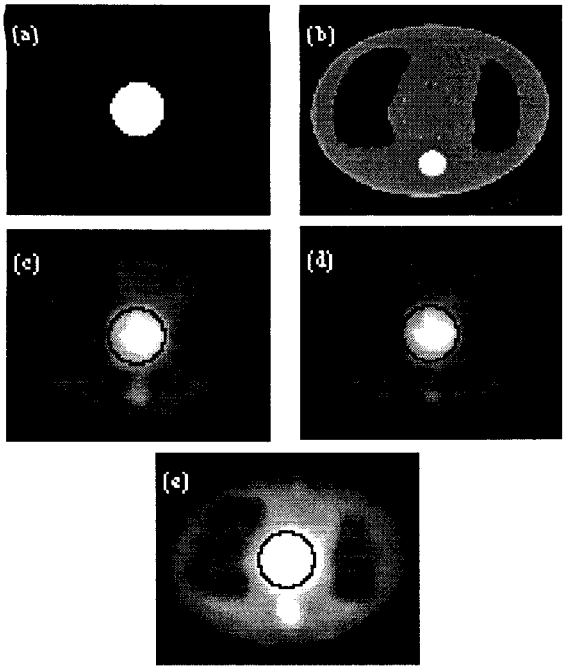

Figure 4: A slice of the lung phantom. (a) True activity (b) X-ray CT image (c) SPECT image reconstructed with no scatter correction (d) SPECT image reconstructed with TEW scatter correction (e) SPECT image of the estimated scatter counts.

over compensation of scatter in the low density lung equivalent medium, or due to object shape and size effects which were not considered here. Reasonable accuracy is achieved even with no scatter correction since in this case also a calibration factor that depends on background activity level was used. Therefore, the uncorrected results presented here have been implicitly compensated for scatter to some extent although no actual scatter subtraction was performed[6]. If a constant calibration factor is to be used irrespective of background activity the TEW correction will result in significantly better accuracy over a range of background levels because of the less severe dependence of CF on b (Figure 2).

Because of partial volume effects the tumor volume outlined on the CT was 15% different from the true volume when 1 cm CT slices were used to define the object. Therefore, the quantification procedure was repeated using 3 mm CT slices to outline the tumor and these results also tabulated in Table 1 are closer to the true activities

The signal to noise ratio, S/N, tabulated is the ratio of total counts in the object to the standard deviation. These numbers show that reconstruction without scatter subtraction gives a better S/N.

C. Preliminary Clinical Results

The quantification procedure with TEW scatter correction described in this work is now being used to evaluate the tumor activity of B-cell lymphoma patients treated with ^{131}I radioimmunotherapy. A reconstructed slice of the neck of a patient with a large tumor is shown in Figure 5 where the high uptake tumor region can be clearly distinguished. The tumor ROI was outlined on the CT and then transferred to the SPECT image. Imaging time was 42 hr after administration of 90 mCi of ^{131}I labeled anti-B1 Mab and data were acquired over 20 min. With TEW scatter correction and using a background dependent calibration factor the tumor activity was determined to be 564 μCi or 0.7% of the decay corrected injected dose. The intensity profile across the trachea with and without scatter correction is also shown in Figure 5.

V. CONCLUSIONS

This work shows that TEW scatter correction for ^{131}I results in reasonable quantitative accuracy and noise characteristics. The difference between TEW scatter corrected and uncorrected ^{131}I images is subtle, but the corrected images are closer to the true activity distribution. The dependence of calibration factor on the background activity level is significantly reduced by TEW scatter correction but still exists because of the finite position resolution of the system. This complicates the clinical quantification procedure since a tumor dependent calibration factor must be used to obtain accurate results. Using a background dependent calibration and TEW

Table 1.
Activity and S/N ratio for lung phantom with TEW correction and no scatter correction. Values in brackets are percentage errors from true activity.

	Activity (uCi)			S/N	
	True	Uncorrected	TEW	Uncorrected	TEW
Using 1 cm CT slices to define object [a]					
Tumor (uniform background)	180.4	192.6 (-6.8%)	190.1 (-5.4%)	6.6	5.4
Tumor (non-uniform background)	118.3	130.9 (-10.6%)	128.3 (-8.4%)	7.7	6.1
Right Lung	195.0	159.5 (18.2%)	167.0(14.4%)	-	-
Using 3 mm CT slices to define object [b]					
Tumor (uniform background)	180.4	187.6 (-4.0%)	185.2 (-2.7%)	6.8	5.3
Tumor (non-uniform background)	118.3	125.1 (-5.7%)	123.5 (-4.4%)	7.8	6.2

a. Results are mean values evaluated from 3 heads
b. Results are for head 1 only

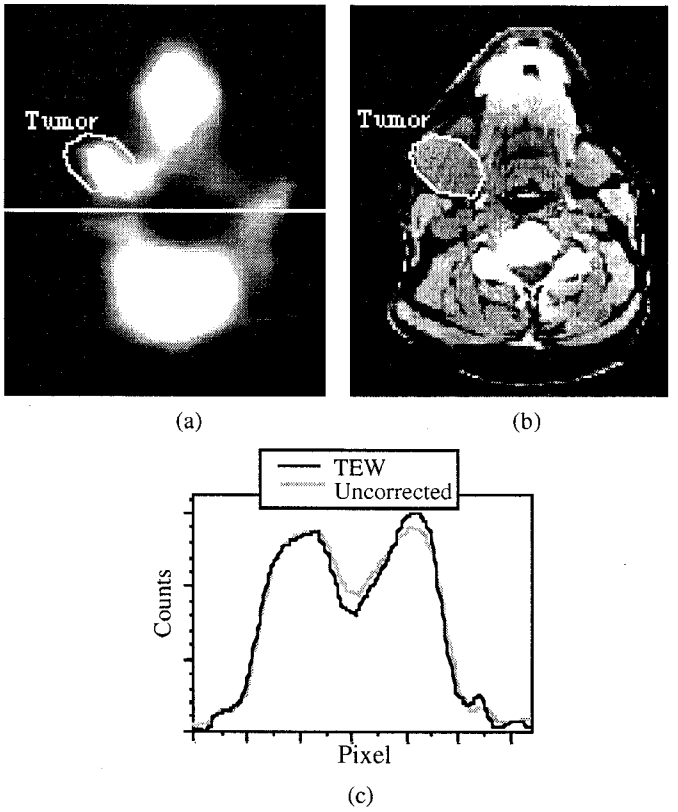

Figure 5:(a) TEW scatter compensated reconstructed slice of a patient neck (b) X-ray CT of the same slice used to define tumor (c) intensity profile across the trachea.

scatter correction quantitative accuracy was 5% and 14% for the tumor and right lung respectively of a physical phantom. With no scatter subtraction but using a background dependent calibration the quantitative accuracy was 7% and 18% for the tumor and lung respectively.

VI. ACKNOWLEDGMENTS

This work was supported by PHS Grant Number R01 CA38790 awarded by the National Cancer Institute, DHHS. Its contents are solely the responsibility of the authors and do not necessarily represent the official views of the National Cancer Institute.

VII. REFERENCES

[1] I. Buvat, M. Rodriguez-Villafuerte, A. Todd-Popropek et al, "Comparative assessment of nine scatter correction methods based on spectral analysis using simulations", *J. Nucl. Med.*, vol. 36(8), pp.1476-88, 1995.

[2] M. Ljungberg, M. King, A. Hademenos et al, "Comparison of four scatter correction methods using Monte Carlo simulated source distributions", *J. Nucl. Med.*, vol. 35(1), pp. 143-51, 1994.

[3] K. R. Pollard, T. K. Lewellen, M. S. Kaplan et al, "Energy-based scatter correction for scintillation camera images of iodine-131", *J. Nucl. Med.*, 37(12), pp.2030-2037, 1996.

[4] K. Ogawa, Y. Harata, T. Ichihara et al, "A practical method for position dependent scatter correction in single photon emission CT", *IEEE Trans. Med. Imag.*, vol. 10(3), pp. 408-412, 1991.

[5] T. Ichihara, K. Ogawa, N. Motomura et al, "Compton scatter compensation using the triple-energy window method for single- and dual-isotope SPECT", *J. Nucl. Med*, vol 34(12), pp. 2216-2221, 1993.

[6] K. Koral, Y. Dewaraja and S. Lin, "^{131}I Tumor quantification: A new background adaptive method", *Proc. IEEE Nuclear Science Symposium and Medical Imaging Conference*, Albuquerque, NM, 1997.

[7] K. Koral, K. Zasadny, M. Kessler et al, "CT-SPECT fusion plus conjugate views for determining dosimetry in I-131-monoclonal antibody therapy of lymphoma patients", *J. Nucl. Med*, vol 35(10), pp. 1714-1720, 1994.

[8] J. Fessler and A. Hero, "Space alternating generalized expectation-maximization algorithm", *IEEE Trans.. Signal Processing*, vol. 42(10), pp. 2664-2677, 1994.